Effect of thermal history on the initiation of slow crack growth in linear polyethylene

Xici Lu* and Norman Brown
Department of Materials Science and Engineering and Laboratory for Research on Structure of Matter, University of Pennsylvania, Philadelphia, PA 19104, USA
(Received 15 August 1986; revised 8 December 1986; accepted 12 January 1987)

Increasing the cooling rate from the melt has been found to increase the rate of slow crack growth at 42°C. For various histories of cooling rate, annealing and specimen geometries, the initiation rate increased when the density decreased. The effect of residual stresses on slow crack growth was separated from the effect of morphology as reflected by density. It is concluded that the variation in yield point is a factor that affects the rate of slow crack growth. The disentanglement rate of fibrils is also important, but it is primarily controlled by molecular weight and branching.

(Keywords: crack growth; thermal history; polyethylene)

INTRODUCTION

The fracture behaviour and yield of polyethylene (PE) is very dependent on its thermal history. Brown and Ward[1] have investigated the influence of morphology on the low temperature brittle fracture strength of PE and found that rapid cooling and high molecular weight increased the fracture stress. These results are consistent with the idea that the number of tie molecules increases with cooling rate and molecular weight and that the fracture stress increases with the number of tie molecules. Mandell, Roberts and McGarry[2] measured the fracture toughness of PE at low temperatures and showed that the plane strain fracture toughness increased with decreasing crystallinity when the crystallinity was varied by cooling rate, by short branches or by molecular weight. Lustiger and Markham[3] have suggested that tie molecules should decrease the rate of slow crack growth in PE at room temperature. Cooney[4] measured the time of brittle failure in PE by slow crack growth and found that a low melt flow index and rapid cooling increased the time to fracture. Cooney used unnotched specimens so that cracks originated at random defects close to the surface. Since rapid cooling generates compressive stresses at the surface, these residual stresses may have reduced the rate of slow crack growth. Hin and Cherry[5], using the same type of PE, found that rapid cooling reduced the time for brittle fracture. The disagreement between the results of Cooney and those of Hin and Cherry may be because Cooney used biaxially bent specimens so that the crack nucleated below the surface of the quenched sheet whereas Hin and Cherry used uniaxial tension specimens so that a crack could nucleate on an inner surface. At the outer surface the residual stress is compressive and at the inner surface a tensile residual stress occurs. The work described here was done to determine the effect of cooling rate on the kinetics of slow crack growth in PE. The initiation stage is emphasized because Lu and Brown[6,7] have shown that the entire process of slow crack growth depends on the rate of initiation and that the initiation rate varies with the fifth power of the stress. Thus, it would appear that residual stresses of a few MPa would have a significant effect. Since cooling rate affects both morphology and residual stress, a special effort was made to separate the two.

It was found that increasing the cooling rate increased the initiation rate. The morphological effect, as reflected by density, prevailed whether or not residual stresses existed.

EXPERIMENTAL

The PE from Phillips Chemical Company was Marlex 6006 used in previous investigations[6,7], with $M_n = 19\,600$, $M_w = 130\,000$, $MI = 0.75$. The resin was compression moulded in a special die which permitted various pressure histories during the thermal history of a specimen. The details of the pressure history during melting have been described[7]. The slow-cooled state was kept in the die under a pressure of 1.7 MPa and cooled overnight. An intermediate cooling rate was produced by cooling the press by its water jacket. Rapid cooling was produced by quenching the die in water. The cooling rate was measured by inserting a thermocouple in the die. The reported cooling rates are an average value measured between about 150 and 120°C.

Most plaques were 4.3 mm thick and some were 7 mm. The geometries of the specimens are shown in *Figure 1*. The samples were notched and tested under three-point bending, the notches being made with a razor blade as described previously[6], with a depth in the range 350–409 μm. After measuring the actual depth to within 4 μm, the results were normalized to a common depth of 400 μm. For all tests, the surface stress was 11 ± 0.05 MPa and the test temperature was 42 ± 0.2°C. In previous investigations[6,7] it was shown that the initiation rate could be reproduced within $\pm 15\%$ for a given stress intensity.

* Visiting Scholar, University of Science and Technology of China, Hefei, People's Republic of China.

0032-3861/87/091505-07$03.00

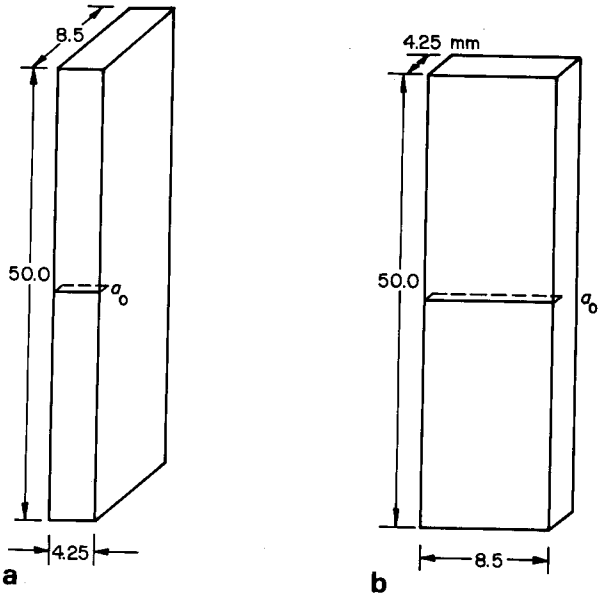

Figure 1 Specimens cut from 4.25 mm thick compression moulded plaques. (a) Average residual stress along side notch equals zero. (b) Residual stress along surface notch is compressive

The density of each specimen was obtained by measuring its weight and volume. Yield points were measured at room temperature at a strain rate of $0.3\ min^{-1}$.

The notch opening was measured with an optical microscope at 200× magnification with a filar eyepiece. The notch opening was measured at the surface of the specimen and at the tip of the notch as defined by the razor blade (*Figure 2*). The error in measuring the notch opening was within $\pm 2\,\mu m$.

The residual stresses were measured by incrementally milling layers of material from one surface and measuring the change in curvature of the specimen. Residual stress was calculated from a plot of curvature vs. thickness of removed layers in accordance with the equations of Russell and Beaumont[9] as derived from the original theory of Treuting and Read[10].

The effect of the residual stresses was eliminated or greatly reduced by annealing at 80°C, by placing the notch so that the residual stresses averaged to zero over the length of the notch or by removing some of the outer surface of the quenched specimen.

RESULTS

Typical behaviour

A typical curve of the opening displacement vs. time is shown in *Figure 3*. The curve has the following features: (a) immediately upon loading the specimen, there is an initial opening displacement δ_0; (b) the initial rate of notch opening, $\dot{\delta}_0$, is nearly constant until crack growth begins at a critical value of $\delta = \delta_c$; and (c) after crack growth occurs, the δ vs. t curve accelerates until the final fracture.

Figure 4 shows the growth of the damage zone prior to and after crack growth. The ratio of δ to the length of the damage zone, α, remains nearly constant during most of the lifetime of the specimen, as shown previously[6,7]. A typical value of α is about 1/7. Initially, the damage zone consists of an array of micro-crazes which grow and form a coarse fibrillar structure. Then, the coarse fibrils break

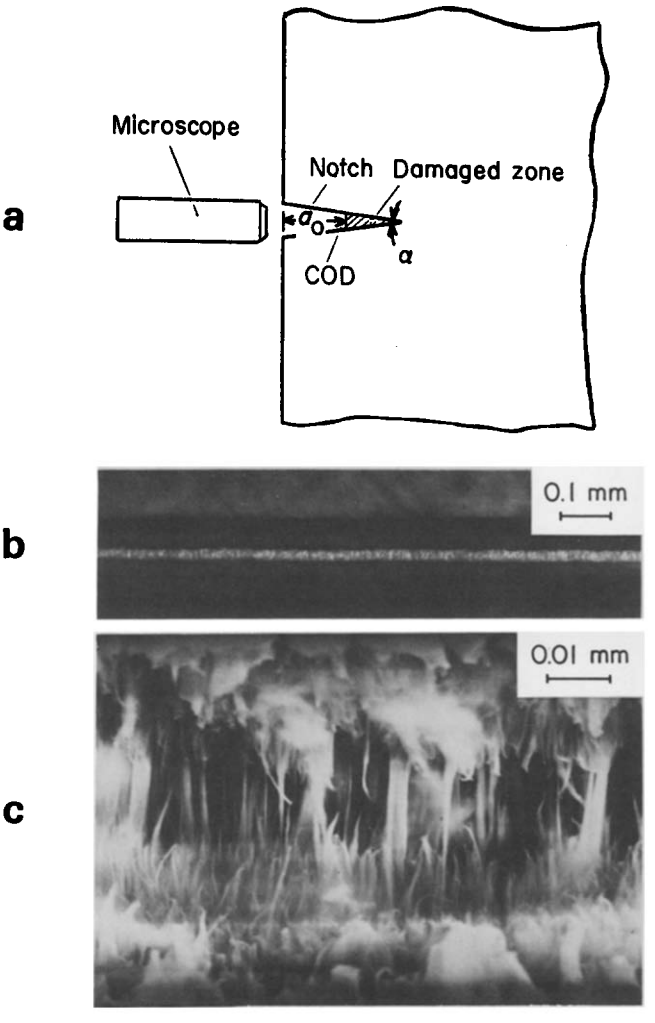

Figure 2 Experimental set-up. (a) Schematic. (b) Notch opening as observed with optical microscope. (c) Notch opening as viewed with SEM

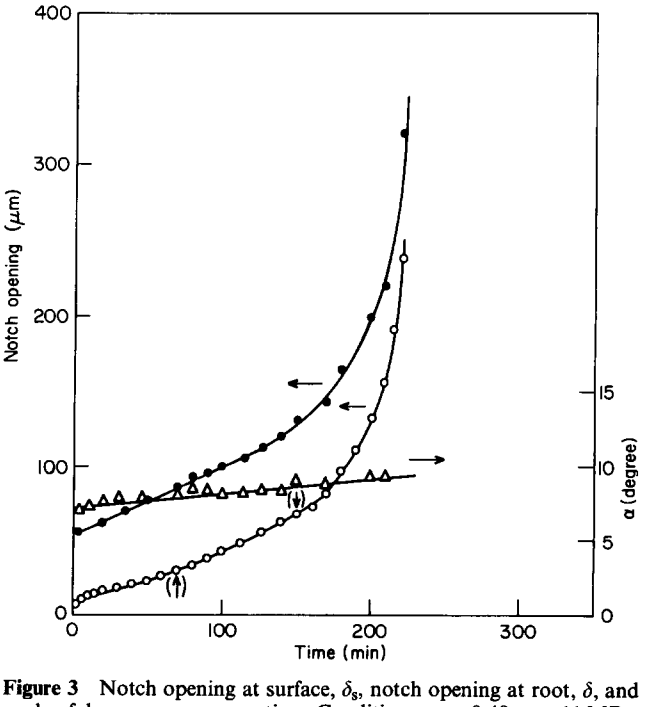

Figure 3 Notch opening at surface, δ_s, notch opening at root, δ, and angle of damage zone, α, vs. time. Conditions: $a_0 = 0.40$ mm; 11 MPa; 42°C. ●, δ_s; ○, COD = δ; △, angle of damage zone, α. ↑, indicates the beginning of fibril fracture; ↓, indicates the breaking of all fibrils at the notch tip

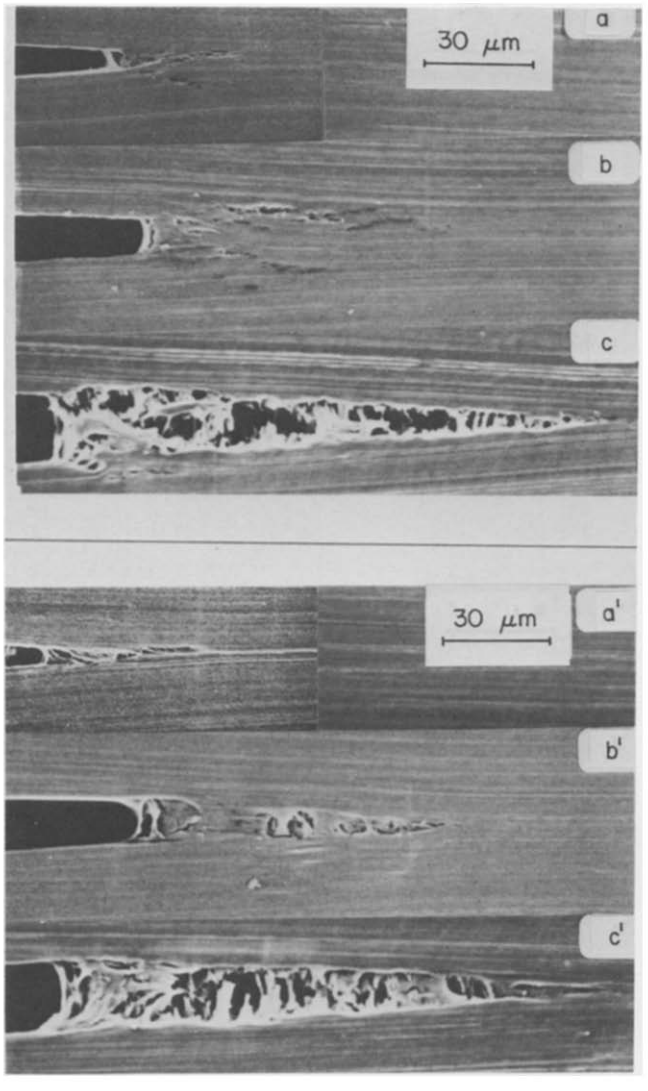

Figure 4 Damage zone for the slow-cooled state after (a)$\delta = 15\,\mu m$, $t = 6.4$ min; (b) $\delta = 25\,\mu m$, $t = 25$ min; (c) $\delta = 40\,\mu m$, $t = 65$ min; and for the quenched state: (a') $\delta = 15\,\mu m$, $t = 2$ min; (b') $\delta = 25\,\mu m$, $t = 3.8$ min; (c') $\delta = 40\,\mu m$, $t = 18$ min. Test conditions: $a_0 = 400\,\mu m$, $\sigma = 11$ MPa, 42°C. Different values of notch depth are shown in each figure

to form the crack. At δ_c, as indicated by the upward arrows in *Figure 3*, fibril fracture starts and, at the point of the downward arrows, a completely fractured surface is observed.

The question arises as to how the curve of δ vs. t (*Figure 3*) should be characterized. It has been shown previously[6,7] that if δ_c, α and the initial notch depth, a_0, and $\dot{\delta}_0$ are known, the part of the δ–t curve beyond δ_c can be calculated from the equation:

$$\dot{\delta}/\dot{\delta}_0 = \left(\frac{a_0 + \delta/\alpha}{a_0 + \delta_c/\alpha}\right)^2 \quad (1)$$

The time to failure can be predicted[7] from:

$$t_f = \alpha a_0/\dot{\delta}_0 \quad (2)$$

Since α, a_0 and δ_c are practically the same for all tests, the most important variable is $\dot{\delta}_0$, the initial rate of damage. Thus, for a fixed stress, temperature and notch depth, $\dot{\delta}_0$ is an experimental rate constant for the slow crack growth phenomenon which should reflect the variation in the morphology of the material.

Lu and Brown[7] have shown for three-point bending that:

$$\dot{\delta}_0 = C\sigma^{5.4} a_0^{1.8} e^{-Q/RT}$$

where C and Q are material parameters. In order to determine the effect of morphology, $\dot{\delta}_0$ was measured at constant σ, a_0 and T.

Effect of cooling rate

Figure 5 shows the general effect of cooling rate on $\dot{\delta}_0$. The faster the cooling rate, the faster the rate of damage. *Figure 6* shows the effect of cooling rate on the stress–strain curve. *Table 1* shows the results for 11 different specimen histories. $\dot{\delta}_0$(av) ranges from 0.44 $\mu m\,min^{-1}$ for the slowest cooling rate to 1.26 $\mu m\,min^{-1}$ for the fastest cooling rate. All tests in *Table 1* were conducted at the same maximum surface stress (11 MPa) and at 42°C. a_0 is nearly the same for all tests, but since a_0 can be accurately measured for each specimen, the values of $\dot{\delta}_0$ were all normalized to a common value, $\dot{\delta}_0$(N), for $a_0 = 400\,\mu m$,

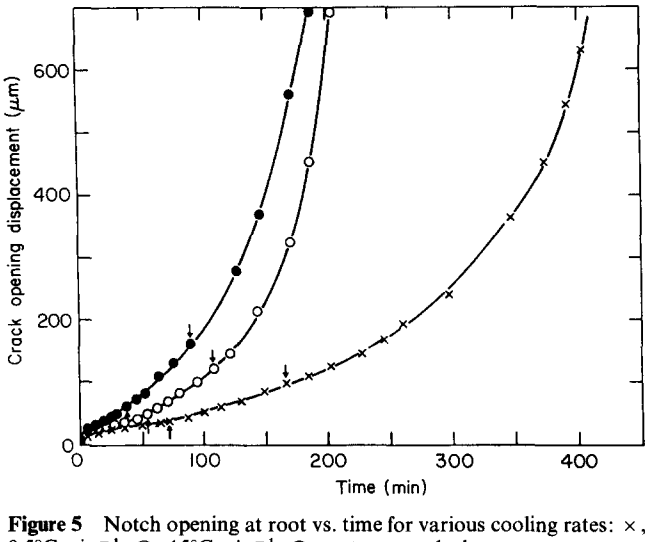

Figure 5 Notch opening at root vs. time for various cooling rates: ×, 0.5°C min^{-1}; ○, 15°C min^{-1}; ●, water quenched

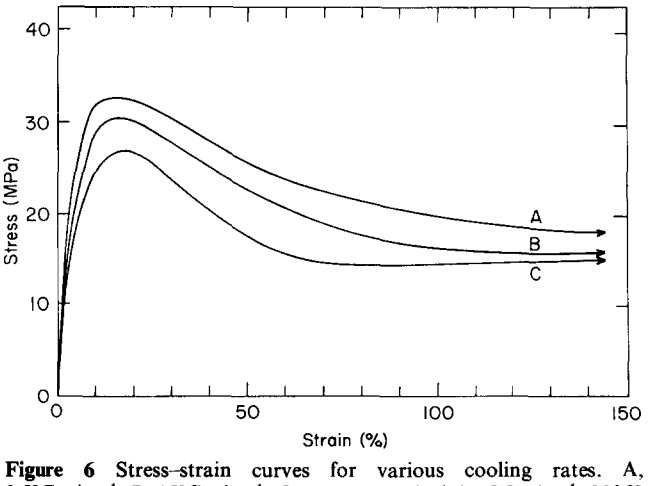

Figure 6 Stress–strain curves for various cooling rates. A, 0.5°C min^{-1}; B, 15°C min^{-1}; C, water quenched. $\dot{\varepsilon} = 0.3\,min^{-1}$, 300 K

Table 1 History of specimens and test results

Test no.	History of specimen	Density (g cm^{-3})	Yield point (MPa)	a_0 (μm)	$\dot{\delta}_0$ (μm min^{-1})	$\dot{\delta}_0$(N) (μm min^{-1})	$\dot{\delta}_0$(av) (μm min^{-1})	δ_0 (μm)
1	Std, SC	0.960	32.2	396	0.49	0.49		13
				386	0.37	0.39	0.44	13
2	SC, pressure = 0 during cooling	0.962		401	0.42	0.42		13
				409	0.42	0.40	0.41	13
3	Cooled 15°C min^{-1}	0.954	30.3	393	0.63	0.65		13
				398	0.70	0.70	0.68	16
4	Q	0.936	25.7	366	1.10	1.29		17
				397	1.22	1.22	1.26	19
5	Q, A2 days, 80°C	0.939	26.6	367	0.91	1.06		17
				393	1.14	1.16	1.11	15
6	Q, A4 days, 80°C	0.941	27.2	399	0.99	0.99		16
				406	1.06	1.03	1.01	14
7	Q, A6 days, 80°C	0.944	27.7	427	0.91	0.82		16
				368	0.83	0.96	0.89	16
8	Q, A8 days, 80°C	0.947	28.0	392	0.81	0.84		16
				402	0.82	0.82	0.83	18
9	Q, 7 mm thick	0.943		358	0.72	0.88		16
				367	0.80	0.93	0.91	18
10	Q, 7 mm thick, 1.5 mm surface layers removed	0.946		356	0.70	0.86		17
				350	0.62	0.79	0.83	18
11	Q, notch along outer surface	0.936	25.7	403	0.93	0.92		14
				400	0.74	0.74	0.83	16

SC = slow cooled at 0.5°C min^{-1}; Q = water quench; A = annealed; a_0 = notch depth; $\dot{\delta}_0$(av) = average value; δ_0 = notch opening at $t = 0$

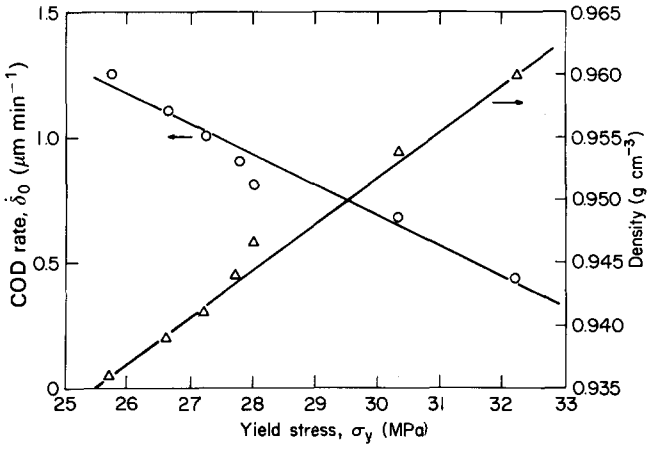

Figure 7 Relationship between $\dot{\delta}_0$, density and yield point

where

$$\dot{\delta}_0(\mathrm{N}) = \dot{\delta}_0\left(\frac{400}{a_0}\right)^{1.8} \tag{3}$$

For each specimen history in *Table 1*, at least two duplicate tests were made. If the maximum difference between two of the tests is $\Delta\dot{\delta}_0(\mathrm{N})$, then the percent scatter may be defined as:

$$S = \frac{\Delta\dot{\delta}_0(\mathrm{N})}{\dot{\delta}_0(\mathrm{av})} \times 100 \tag{4}$$

where $\dot{\delta}_0(\mathrm{av})$ is the average value. The average value of S from all tests in *Table 1* is 10%. Thus, it is estimated that the values of $\dot{\delta}_0(\mathrm{av})$ are significant within about $\pm 10\%$. This estimate of the scatter is consistent with the results of the previous investigations[6,7], where the scatter in $\dot{\delta}_0$ was within $\pm 15\%$ for a given value of the stress intensity.

A general effect of cooling rate is that density decreases with increasing cooling rate. Also, the yield point decreases with decreasing density. *Table 1* shows that $\dot{\delta}_0(\mathrm{av})$ decreases with increasing density for all but one specimen history. *Figure 7* shows the relationship between $\dot{\delta}_0$, σ_y and density.

Table 1 shows that the initial value of the notch opening, δ_0, increases with decreasing density and yield point. From the Dugdale theory:

$$\delta_0 = \frac{K^2}{\sigma_y E(1-\nu^2)} \tag{5}$$

where K is stress intensity, E is modulus and ν is Poisson's ratio. Previous work has shown that $\sigma_y = 0.022E$. Thus, δ_0 varies inversely with σ_y^2, as shown in previous investigations[6,7]. With $\nu = 0.4$ and $K = 0.4\,\mathrm{MPa\,m^{1/2}}$ and $\sigma_y = 27$ MPa, $\delta_0 = 6\,\mu$m, which is appreciably smaller than the values in *Table 1*. Part of the discrepancy probably arises from the fact that the values of δ_0 in *Table 1* were obtained by linear extrapolation back to $t = 0$ whereas the curves (*Figures 3* and *5*) all indicate non-linear behaviour near $t = 0$.

Annealing after quenching

Tests 4–8 in *Table 1* show the effects of annealing the quenched state at 80°C. *Figure 8* is a plot of density and residual stress vs. annealing time. The density continues to increase with annealing time after the residual stress disappears. $\dot{\delta}_0$ continues to decrease as the density increases with annealing time. This supports the conclusion that it is primarily the morphological change as reflected by density that influences $\dot{\delta}_0$.

Effects of the residual stress

The following tests were done in order to explore the effect of residual stress on $\dot{\delta}_0$. Figure *9* shows the residual stress distribution after quenching the 4.3 mm thick plaque. The residual stress is compressive on the outside

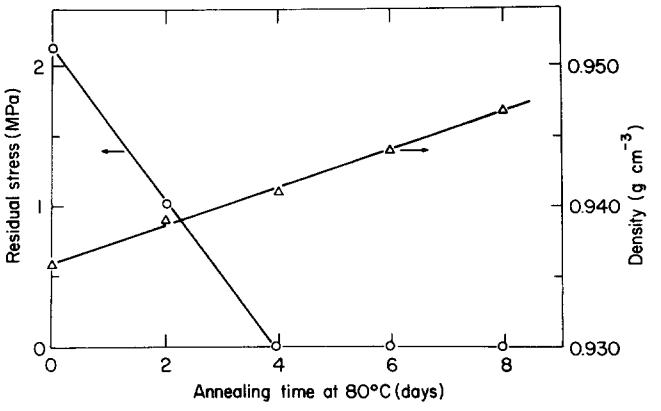

Figure 8 Density and compressive residual stress at surface vs. annealing time at 80°C

because the inside crystallizes after the outside crystallizes, and the shrinkage on the inside during crystallization puts the outside into compression. The residual stresses show a maximum value of −2.2 MPa on the outer surface and reduce to about −1.1 MPa at a depth of 0.4 mm. Tests 4 and 11 have the same thermal history except that the notch in test 4 (*Figure 1a*) experiences an average residual stress of zero and the notch in test 11 (*Figure 1b*) experiences a residual stress of −1.1 MPa. $\dot{\delta}_0 = 1.26$ for test 4 and 0.83 for test 11. Thus, as expected, the compressive residual stress does decrease $\dot{\delta}_0$, depending on the placement of the notch.

Effect of specimen thickness

A 7 mm thick specimen was compared with a 4 mm specimen. For the slow-cooled state, thickness has no effect. For the quenched states (compare tests 4 and 9), the thinner specimen cools more rapidly so that its density is 0.936 compared with 0.943 for the thicker one; the corresponding values of $\dot{\delta}_0$ are 1.26 and 0.91.

In test 10, a 1.5 mm layer of material was milled from each surface of the original 7 mm thick quenched specimen. $\dot{\delta}_0$ for test 10 is 0.83 compared with 0.91 for test 9, which is the state prior to milling. The decrease in $\dot{\delta}_0$ after milling is expected because the remaining material cools more slowly than the outer layer and therefore the average density of the specimen is increased.

Effect of moulding procedure

The standard slow-cooled specimen is crystallized under a pressure of 1.7 MPa. In order to quench the material it is necessary to remove the pressure prior to quenching. Therefore, the effect of pressure on the slow-cooled material was investigated by reducing the pressure to about zero during crystallization. A comparison of tests 1 and 2 shows that the difference in pressure has practically no effect on density or $\dot{\delta}_0$. Therefore, the lack of pressure during quenching probably has little or no effect on the difference between the slow-cooled and quenched states.

DISCUSSION

The results show that $\dot{\delta}_0$ increases with decreasing density where the density has been changed by varying the quenching rate, specimen thickness and annealing time. The effect of residual stress only manifested itself if the average residual stress along the notch was not zero. When the residual stress along the notch tip was about −1.1 MPa, $\dot{\delta}_0$ was reduced from 1.26 to 0.83 (tests 4 and 11, respectively), but even with a net residual stress along the notch, the value of 0.83 for the quenched state is double the value of 0.44 for the slow-cooled material in test 1.

Since $\dot{\delta}_0 \sim \sigma^{5.4}$, as shown previously[7], the effect of the residual stress on $\dot{\delta}_0$ in test 11 is reasonable. In comparing tests 4 and 11, the ratio of the stresses is $11/(11-1.1)$, if −1.1 is the residual stress. Thus the calculated ratio of $\dot{\delta}_0(4)/\dot{\delta}_0(11) = (11/9.9)^{5.4} = 1.8$. The experimental value of $\dot{\delta}_0(4)/\dot{\delta}_0(11) = 1.5$. The agreement is reasonable. The effect of the residual stress is measurable and can be separated from the effect of morphology as reflected by the density.

The primary effect of the cooling rate on $\dot{\delta}_0$ is associated with the morphological change that is reflected by the density. We suggest that considerations of the effect of the yield point may be a more direct way of understanding the correlation between $\dot{\delta}_0$ and density. An equation for $\dot{\delta}_0$ has been proposed[7] based on the growth of the micro-crazes within the damage zone where:

$$\dot{\delta}_0 = \frac{K^2 \dot{b} \rho^{1/2} \beta^{1/2}}{\sigma_y E(1-\nu^2)} \tag{6}$$

where K is the stress intensity, $\dot{b}$ is the growth rate of a micro-craze, ρ is the density of micro-crazes per unit area of the damage zone, β is a shape factor for a micro-craze, σ_y is yield point, E is Young's modulus and ν is Poisson's ratio. The above equation states $\dot{\delta}_0$ varies inversely as σ_y^2 since E is proportional to σ_y. However, $\dot{b}$ and ρ may also

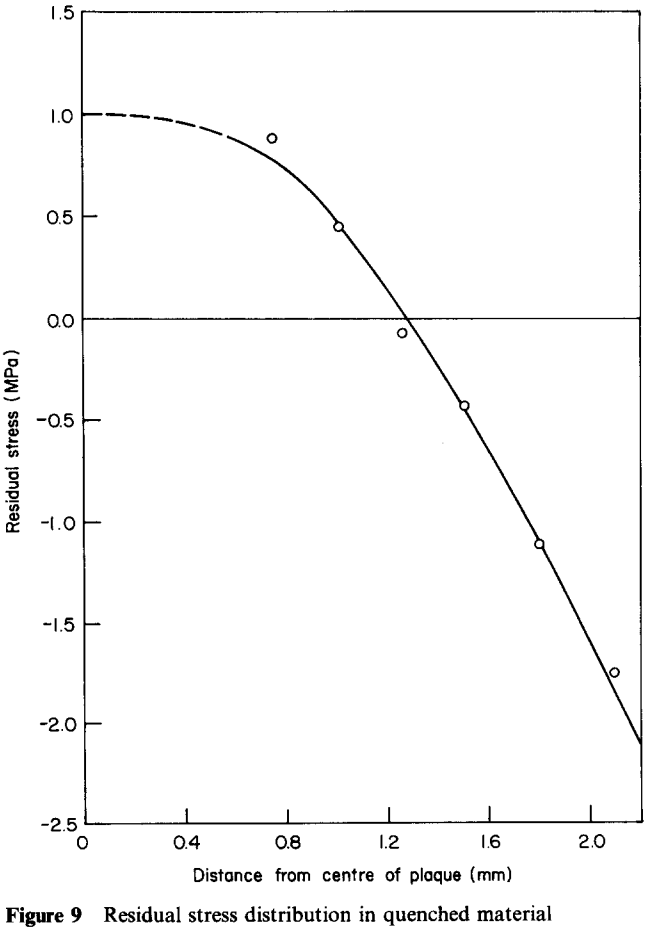

Figure 9 Residual stress distribution in quenched material

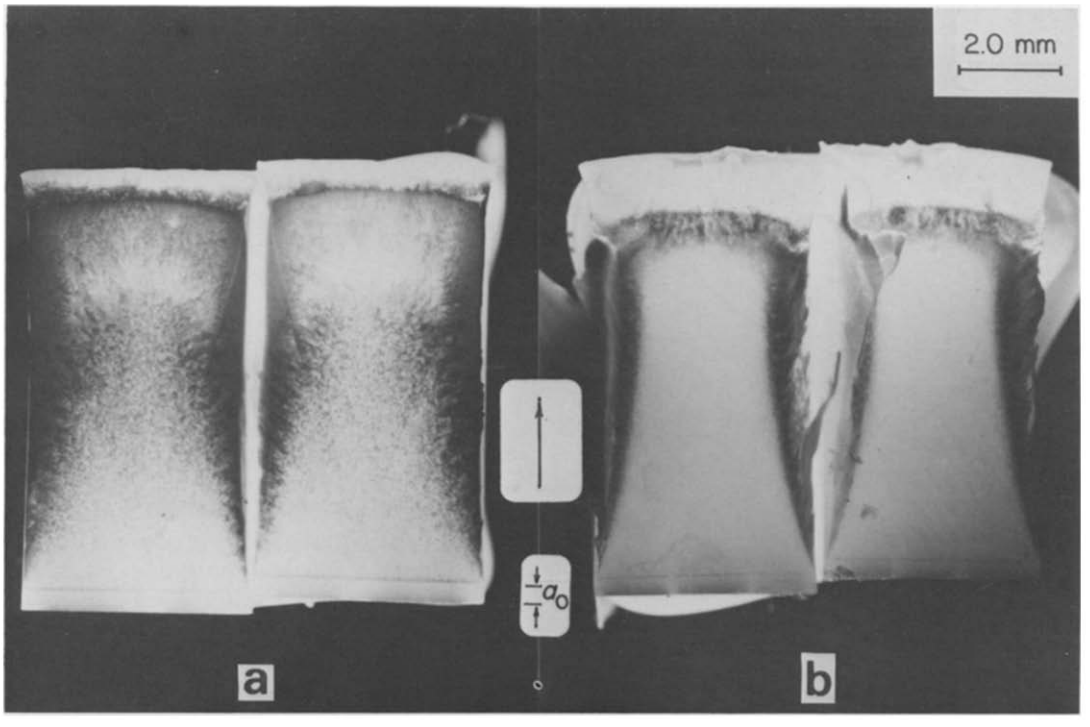

Figure 10 Optical micrograph of fractured surfaces of: (a) slow-cooled and (b) quenched state. The slow-cooled state has a rougher surface. The arrow shows crack growth direction. a_0 is the notch length

depend on σ_y so that the dependence of $\dot{\delta}_0$ on σ_y may be greater than suggested by the above equation. Experimentally[7] it was determined that $\dot{\delta}_0 \sim \sigma^{5.4}$. If the above relationship were normalized relative to the yield point so that $\dot{\delta}_0 \sim (\sigma/\sigma_y)^{5.4}$ then the ratio of $\dot{\delta}_0$ for the slow cooled and quenched state can be estimated where $\dot{\delta}_0(1)/\dot{\delta}_0(4) = (32.2/25.7)^{5.4} = 3.4$. The experimental value of $\dot{\delta}_0(1)/\dot{\delta}_0(4) = 1.26/0.44 = 2.9$. The agreement is good. The above considerations lead to the conclusion that the higher the yield point the lower is $\dot{\delta}_0$.

Figure 10 shows the fractured surfaces of the slow-cooled and quenched materials. The slow-cooled material has a rougher surface than that of the quenched one. This suggests that more energy was required to produce a unit area of the fractured surface of the slow-cooled state. Consequently, it is expected that $\dot{\delta}_0$ will be less for the slow-cooled state.

When one studies many micrographs, such as those in *Figure 4*, it appears that the growth of the damaged zone involves two processes: (1) there is a yield process on the boundary of the damaged zone which converts the bulk material to the yield state; and (2) there is a growth of micro-crazes within the damaged zone. It is suggested that the enlargement of the boundary is controlled by the yield point and the micro-craze enlargement involves the disentanglement of fibrils. The disentanglement process is also very important, as evidenced by the many investigations, such as those of Cooney[4] and Bubeck and Baker[8] that an increase of molecular weight decreases the rate of slow crack growth. Short branches such as in butene and hexene copolymers are also very important in determining the rate of slow crack growth. The branching and molecular weight effects are distinct from the density effect in that both branching and higher molecular weight decrease the density for a given cooling rate.

Thus, the three aspects of structure that control the process of slow crack growth are density, molecular weight and branching. In the light of equation (6), density is involved through σ_y and E; $\dot{b}$, the rate of enlargement of micro-crazes, is related to molecular weight and branching. Whereas $\dot{b}$ may decrease continuously with increasing molecular weight, there may be an optimum amount of branching that produces a minimum in $\dot{b}$.

Brown and Ward[1] have measured the low-temperature brittle fracture stress of slow-cooled and quenched material and found that the fracture stress is greater for the quenched state. Mandell *et al.*[2] found that the low temperature fracture toughness increased when the density of the PE was decreased. We find that at room temperature the rate of slow crack growth is increased by quenching. We attribute this difference in fracture resistance to the difference between the fracture processes at low temperature and at room temperature. At very low temperatures, brittle fracture occurs primarily by scission of the molecules within the amorphous region. Since fracture occurs prior to yield, the tie molecules introduced by quenching are important. At room temperature, disentanglement of molecules in fibrils is the mode of fracture. Since disentanglement requires the prior nucleation of micro-crazes which depends on the yield point, morphological changes associated with the yield point are important at room temperature. It has been suggested[3] that tie molecules decrease the disentanglement rate, but if quenching increases the number of tie molecules, and at the same time increases $\dot{\delta}_0$, it would mean that the yield point effect dominates the tie molecule effect for linear PE having this particular molecular weight.

The required molecular mobility for the disentanglement process is expected in PE at room temperature because room temperature is about 0.78 times the melting point of PE. In all crystals above 0.5 times the melting point, the atomic or molecular mobility becomes significant, so that diffusion-controlled creep processes

can occur[11]. Also, room temperature is above T_g for the amorphous region so that a portion of the PE is essentially in the liquid-like state. It is anticipated that for all crystalline polymers at temperatures above about 0.7 of the melting point, slow crack growth will be an important mode of failure at low stresses.

CONCLUSIONS

(1) The rate of initiation and rate of failure by slow crack growth increase with cooling rate.

(2) The effect of residual stresses is separable from the effects of morphology, as reflected by the density.

(3) In general, the rate of initiation increases with decreasing density which, in turn, controls the yield point.

(4) The higher the yield point the lower the initiation rate for slow crack growth in linear PE.

(5) The rate of disentanglement of fibrils, which is mostly controlled by molecular weight and branching, is also important in addition to the yield point.

ACKNOWLEDGEMENTS

This research was supported by the Gas Research Institute and the US Department of Energy. The Central Facilities of the Materials Research Laboratory were very helpful. The experimental assistance of Ms X. Q. Wang is also much appreciated.

REFERENCES

1 Brown, N. and Ward, I. M. *J. Mater. Sci.* 1983, **18**, 1405
2 Mandell, J. F., Roberts, D. R. and McGarry, F. J. *Polym. Eng. Sci.* 1983, **23**, 404
3 Lustiger, A. and Markham, R. L. *Polymer* 1983, **24**, 1647
4 Cooney, J. L. *J. Appl. Polym. Sci.* 1964, **8**, 1889
5 Hin, T. S. and Cherry, B. W. *Polymer* 1984, **25**, 727
6 Lu, X. and Brown, N. *J. Mater. Sci.* 1986, **21**, 2217
7 Lu, X. and Brown, N. *J. Mater. Sci.* 1986, **21**, 4081
8 Bubeck, R. A. and Baker, H. M. *Polymer* 1982, **23**, 1680
9 Russell, D. P. and Beaumont, P. W. R. *J. Mater. Sci.* 1980, **15**, 208
10 Treuting, R. G. and Read, W. T. Jr *J. Appl. Phys.* 1951, **22**, 130
11 Dorn, J. E. (Ed.), 'Mechanical Behavior of Materials at Elevated Temperatures', McGraw-Hill, New York, 1961